


ORIGINAL PAPER

The different mechanisms of peripheral and central TLR4 on chronic postsurgical pain in rats

Xuemin Han^{1,3,6} | Jinping Shao^{2,4} | Xiuhua Ren^{2,4} | Yaru Li^{1,3} | Wenli Yu^{2,4} |
Caihong Lin^{2,4} | Lei Li^{2,4} | Yanyan Sun^{2,4} | Bo Xu⁵ | Huan Luo⁷ | Changlian Zhu⁸ |
Jing Cao^{2,4}  | Zhisong Li^{1,3}

¹The Second Affiliated Hospital of Zhengzhou University, Zhengzhou, China

²Department of Human Anatomy, School of Basic Medicine, Zhengzhou University, Zhengzhou, China

³The First Affiliated Hospital of Zhengzhou University, Zhengzhou, China

⁴Institute of Neuroscience, Zhengzhou University, Zhengzhou, China

⁵Department of Anesthesiology, General Hospital of Southern Theatre Command of PLA, Guangzhou, China

⁶Children's Hospital of Soochow University, Soochow, China

⁷Klinik für Augenheilkunde, Charité–Universitätsmedizin Berlin, corporate member of Freie Universität Berlin, Humboldt-Universität zu Berlin, and Berlin Institute of Health, Germany

⁸Center for Brain Repair and Rehabilitation, Institute of Neuroscience and Physiology, Gothenburg University, Gothenburg, Sweden

Correspondence

Zhisong Li, The Second Affiliated Hospital of Zhengzhou University, Zhengzhou 450014, China.
Email: lzszyd@126.com

Jing Cao, Department of Human Anatomy, Zhengzhou University, Number 100 Science Road, Zhengzhou 450001, China.
Email: caojing@zzu.edu.cn

Funding information

This work was supported by the National Natural Science Foundation of China (No. 81671091, 81671094, 61773130).

Abstract

Chronic postsurgical pain (CPSP) is a common complication after surgery; however, the underlying mechanisms of CPSP are poorly understood. As one of the most important inflammatory pathways, the Toll-like receptor 4/nuclear factor-kappa B (TLR4/NF-κB) signaling pathway plays an important role in chronic pain. However, the precise role of the TLR4/NF-κB signaling pathway in CPSP remains unclear. In the present study, we established a rat model of CPSP induced by skin/muscle incision and retraction (SMIR) and verified the effects and mechanisms of central and peripheral TLR4 and NF-κB on hyperalgesia in SMIR rats. The results showed that TLR4 expression was increased in both the spinal dorsal horn and dorsal root ganglia (DRGs) of SMIR rats. However, the TLR4 expression pattern in the spinal cord was different from that in DRGs. In the spinal cord, TLR4 was expressed in both neurons and microglia, whereas it was expressed in neurons but not in satellite glial cells in DRGs. Further results demonstrate that the central and peripheral TLR4/NF-κB signaling pathway is involved in the SMIR-induced CPSP by different mechanisms. In the peripheral nervous system, we revealed that the TLR4/NF-κB signaling pathway induced upregulation of voltage-gated sodium channel 1.7 (Nav1.7) in DRGs, triggering peripheral hyperalgesia in SMIR-induced CPSP. In the central nervous system, the TLR4/NF-κB signaling pathway participated in SMIR-induced CPSP by activating microglia in the spinal cord. Ultimately, our findings demonstrated that activation of the peripheral and central TLR4/NF-κB signaling pathway involved in the development of SMIR-induced CPSP.

KEYWORDS

chronic postoperative pain, microglia, Nav1.7, NF-κB, skin/muscle incision and retraction, TLR4

1 | INTRODUCTION

Chronic postsurgical pain (CPSP) is a widespread clinical problem that can occur following various types of surgery, and is most common following thoracotomies, inguinal hernia repair, and coronary artery bypass surgery (Macrae, 2008). An epidemiological survey showed that approximately 10%–50% of postoperative acute pain converts to CPSP (Kehlet et al., 2006). Furthermore, the incidence of CPSP is increasing each year as a result of the rapid expansion in the number of surgeries worldwide. CPSP has detrimental effects on physical and psychological health as well as daily life. Unfortunately, the pathogenic mechanisms underlying CPSP remain unclear, and the clinical treatment of CPSP is still limited. Therefore, it is important to further elucidate the molecular mechanisms of CPSP to develop improved treatments for CPSP patients.

In recent years, neuroinflammation has been revealed to be an important mechanism in chronic pain that is caused by changes in neural plasticity (Ji et al., 2014). As one of the most important inflammatory pathways, the Toll-like receptor 4/nuclear factor-kappa B (TLR4/NF- κ B) signaling pathway plays an important role in chronic pain by generating and releasing a wide variety of pro-inflammatory factors (Bai et al., 2014; Xu et al., 2018). However, the mechanisms of the TLR4/NF- κ B signaling pathway in CPSP are still unclear.

In the central nervous system, TLR4 is mainly expressed in microglia and is involved in the activation of microglia, which play a crucial role in the process of neuroinflammation within the central nervous system. TLR4 in the spinal cord is also a key factor in neuropathic pain (Iwasaki et al., 2013; Raghavendra et al., 2003). Hence, we hypothesize that TLR4 in the spinal cord participates in hyperalgesia by activating microglia in CPSP.

Interestingly, in chronic pain, TLR4 is expressed not only in the spinal cord of the central nervous system (Bai et al., 2014; Xu et al., 2018), but also in dorsal root ganglia (DRGs) of the peripheral nervous system (Bruno et al., 2018; Xing et al., 2018). The preliminary experimental results of this study showed that, unlike the distribution in the central nervous system, TLR4 was expressed in neurons but not satellite glial cells within DRGs. This suggests that TLR4 may not be involved in regulating pain by activating glia in the peripheral nervous system. Therefore, we speculate that the mechanisms by which TLR4 functions in the central and peripheral nervous systems may be different in CPSP.

Studies have shown that NF- κ B increases neuronal excitability by regulating the expression of voltage-gated sodium channel 1.7 (Nav1.7) in DRG neurons (Huang et al., 2014; Qu et al., 2019; Xie et al., 2019). NF- κ B is an important downstream molecule of the TLR4 signaling pathway. Furthermore, Nav1.7 plays a vital role in initiating action potentials in response to depolarization of sensory neurons by noxious stimuli (Cox et al., 2006; Dib-Hajj et al., 2008). Therefore, we hypothesize that TLR4 is involved in CPSP by regulating the expression of Nav1.7 in the peripheral nervous system.

To test our above hypotheses, in the present study, we established a rat model of CPSP induced by skin/muscle incision

and retraction (SMIR). We investigated the relationship between TLR4/NF- κ B and the activation of microglia in the spinal cord of SMIR rats and revealed that TLR4-activated microglia in SMIR-induced CPSP. In the peripheral nervous system, we found a regulatory relationship between TLR4 and Nav1.7, and demonstrated that TLR4 can upregulate expression of Nav1.7 in SMIR-induced CPSP.

2 | MATERIALS AND METHODS

2.1 | Animals

Male Sprague–Dawley rats (200–250 g) were purchased from the Animal Center of Henan Province. Animals were kept and bred freely within separate cages in a pathogen-free environment, under a standard temperature ($23 \pm 2^\circ\text{C}$) and 12:12-h light-dark cycle. All the animals were randomly divided into groups. All of the experiments were conducted in accordance with protocols approved by the National Institutes of Health on animal care and the ethical guidelines for experimental investigations.

2.2 | Skin/muscle incision and retraction (SMIR)

A model of SMIR was produced in rats according to the methods of a previous study (Flatters, 2008). Rats were anesthetized with chloral hydrate (10%; 400 mg/kg; i.p.) and were shaved at the right medial thigh. The saphenous vein was visualized after swabbing the shaved skin repeatedly with sterile alcohol (75%). Then, an incision (1.5–2.0 cm) was made in this area at approximately 4 mm medial to the saphenous vein to reveal the gracilis muscle of the thigh. The gracilis layer was then subjected to an incision (7–10 mm) and was parted bluntly at approximately 4 mm medial to the saphenous nerve. A micro-dissecting retractor was inserted into this incision site—with all prongs underneath the gracilis layer—to retract the skin and gracilis by up to 2-cm long; then, the underlying adductor muscles were revealed. This retraction was maintained for 1 h. The incision was covered with a wet gauze during the retraction. After these procedures, the surgical site was sutured with 4-0 silk. The sham control underwent only skin incisions without muscle retraction.

2.3 | Behavioral tests

All behavioral tests were double-blind. Mechanical sensitivity was tested with von-Frey hairs, according to the "up-down" method, by applying mechanical stimuli to the plantar surface of the hind paw consisting of an 8-s application or until a response occurred (Chaplan et al., 1994). The 50% paw withdrawal threshold (PWT) was determined according to the "up-down" method in an ascending order of force until a paw withdrawal response was elicited. All rats were

acclimated to the testing environment for at least 30 min before measurements. The interstimulus interval was 5 min. A positive response to the stimulus was assessed by a quick withdrawal and/or licking of the paw.

Thermal hyperalgesia was evaluated by the paw withdrawal latency according to previously reported method (Hargreaves et al., 1988). The plantar surface of the hind paw was stimulated by a radiant heat source beneath a glass floor. The hind paws were tested in alternation. The intervals between consecutive tests were >5 min. The measurements were repeated three times on each side and the mean value was taken. To avoid tissue damage, when the rats had no positive reactions, the radiant heat source was automatically stopped for 20 sec.

2.4 | Catheter implantation

The procedures of intrathecal (i.t.) catheter implantation were performed according to a previous study (Shao et al., 2016; Størkson et al., 1996). Rats were anesthetized with chloral hydrate (10%, 400 mg/kg, i.p.), and then, a skin incision was made in the midline lumbar region (L5–L6). A 23-gauge needle was used to puncture the muscle to access the vertebra. A sterilized polyethylene catheter (PE-10, 18 ± 2 cm) was introduced into the subarachnoid space. A sudden movement of the tail and/or hindlimb indicated dural penetration. The catheter was then pushed gently upward to reach the rostral level of the lumbar enlargement (L4), and was fixed into the superficial muscle by suturing a bead made on the catheter. The catheter was tunneled under the skin and pulled out at the neck, where another skin incision was made and the second bead was fixed into the muscle. Finally, both incisions were then sutured with 4-0 silk. The rats were allowed to recover for a minimum of 7 d. Then, the catheter placement was verified by observing transient hind paw paralysis induced by an injection of lidocaine (2%, 5 µl). Rats exhibiting post-operative neurological deficits (e.g., paralysis) were excluded from subsequent experiments.

2.5 | Drugs and drug delivery

A lipopolysaccharide derived from *Rhodobacter sphaeroides* (LPS-RS) (InvivoGen, San Diego, CA) was injected (2.0 µg/µl, 10 µl, i.t.) intrathecally at 1 d before surgery and once daily thereafter for 10 d to inhibit the TLR4 function. The LPS (InvivoGen, San Diego, CA) was injected twice intrathecally to activate TLR4. For the first injection, all rats received LPS with the same dose (0.2 µg/µl, 10 µl, i.t.) to prime the immune system. A second intrathecal injection was administered with an increasing dose of lipopolysaccharide (LPS) (0.5, 1, and 2 µg/µl, 10 µl, i.t.), followed by a 10 µL saline flush. The NF-κB inhibitor, pyrrolidine dithiocarbamic acid (PDTC) (Sigma, St. Louis, MO), was intrathecally injected at 1 d before surgery and once daily thereafter for 10 d (at 0.05 µg/µl, 10 µl, i.t.).

2.6 | Western blotting

All of the rats were deeply anesthetized using a lethal dose of chloral hydrate (10%; 600 mg/kg; i.p.) at designated time points. The ipsilateral L4–5 DRG and spinal dorsal horn tissues were dissected. Based on established protocol (Shao et al., 2016), all samples were then homogenized in ice-cold cytoplasmic lysis buffer (lysis buffer A: 85.52 mg/ml sucrose, 10 mmol/L Tris, 5 mmol/L MgCl₂, 5 mmol/L EGTA, 0.1 mmol/L PMSF, 0.01 mmol/L DTT, 40 µmol/L leupeptin, 10 mmol/L, and 1% phosphatase inhibitor buffer A and buffer B). Then, the homogenate sample was centrifuged at 2,000 rpm for 15 min at 4°C, after which the supernatant was collected to isolate membrane-bound protein samples. The precipitate containing nuclear protein was added to a nuclear buffer (buffer B: 10 mM Tris, 1.5% SDS, and 0.5% Triton X-100). The samples were centrifuged and collected after being subjected to ultrasound-induced breakage. Protein samples were dissolved in loading buffer and denatured at 99°C for 5 min after measurement of total protein concentrations. Subsequently, 30–60 µg of protein was separated using 10% of sodium dodecyl sulfate (SDS)-polyacrylamide gel electrophoresis (PAGE) and was then transferred onto a polyvinylidene difluoride (PVDF) membrane. The membranes were blocked in TBST with 5% of fat-free milk solution for 2 h at room temperature and were incubated overnight at 4°C with an anti-Nav1.7 antibody, anti-CD11b antibody, anti-TLR4 antibody, anti-p-p65 antibody, or β-actin antibody. The western blotting were then incubated with horseradish peroxidase-conjugated anti-mouse or anti-rabbit secondary antibody. Protein bands were visualized using chemiluminescent reagents with an ECL kit (Sangon Biotech, China), followed by exposure with FluorChem ProteinSimple (AlphaMager ProteinSimple, San Jose, USA). The immunoreactive densities were analyzed with an AlphaView SA analyzer. The optical density was determined by the ratio of the protein signals to β-actin or H3 signal. These ratios were normalized to the control values. The following primary antibodies were used: rabbit anti-phospho-p65-Ser346 (1:1000; Cell Signaling Technology, USA), rabbit anti-Nav1.7 (1:1000; Millipore, USA), rabbit anti-CD11b (1:500; ABclonal, USA), mouse anti-TLR4 (1:200; Abcam, England), rabbit anti-H3 (1:1000; Abcam, England), and mouse anti-β-actin (1:10000; Sigma, UAS).

2.7 | Quantitative real-time PCR

Total RNA from the ipsilateral L4–5 DRG and spinal dorsal horn was extracted with TRIzol (Sangon Biotech, China), as described previously (Su et al., 2017). cDNA synthesis was performed by reverse transcription using the RevertAid-TM First Strand cDNA Synthesis Kit (Thermo Fisher, USA). Quantitative real-time PCR (qRT-PCR) was conducted in triplicate with an ABI-Prism 7500 sequence detection system (Applied Biosystems, USA). The Maxima SYBR Green qPCR MM (Thermo Fisher, USA) was used to detect mRNA. PCR was performed at 50°C for 2 min, followed by 40 cycles at 95°C for 10 min, 95°C for 15 s, and 60°C and 60 s for extension. All reactions were

performed in triplicate in a final volume of 20 μ l. β -actin was used as an internal reference. The relative level of mRNA expression was calculated using the comparative $2^{-\Delta\Delta C_t}$ method.

The primer sequences were as follows:

- SCN9A forward: 5'-GCTCAAAGAGTGCCAAGGAG-3',
- SCN9A reverse: 5'-TTCGGATGCTTTCCTCTGAT-3',
- TLR4 forward: 5'-TGGCATCATCTTCATTGTCC-3',
- TLR4 reverse: 5'-CAGAGCATTGTCCTCCCACT-3',
- CD11b forward: 5'-GTGCTACCTATTCGGCTCCA-3',
- CD11b reverse: 5'-CCGTCAATCAAGAAGGCAAT-3',
- β -actin forward: 5'-GACGATATCGCTGCGCTG-3', and
- β -actin reverse: 5'-GTACGACCAGAGGCATACAGG-3'.

2.8 | Immunofluorescence

Immunofluorescence was performed as previously described (Li et al., 2019; Xu et al., 2006). Briefly, rats were deeply anesthetized with chloral hydrate (10%, 600 mg/kg, i.p.) and perfused through the ascending aorta with heparinized saline, followed by 4% of paraformaldehyde in 0.1 mol/L of phosphate buffer. Then, the ipsilateral L4–5 DRGs and the lumbar (L4–5) spinal cord were removed and postfixed in the same fixative for 3 h, after which the fixative was replaced with 30% of sucrose in phosphate-buffered saline over the course of two nights. Longitudinal DRG sections (16 μ m) and transverse spinal sections (25 μ m) were cut on a cryostat. Then, the sections were blocked with 3% of fetal bovine serum in 0.3% of Triton X-100 (Sigma, St. Louis, MO) for 1 h at room temperature before being incubated overnight at 4°C with primary antibodies. Subsequently, the sections were incubated with a mixture of Cy3- and Cy2-conjugated secondary antibodies for 1 h at 37°C. The primary antibodies that were used included mouse antibodies against TLR4 (1:100; Abcam, England), rabbit anti-phospho-p65 (1:200; Cell Signaling Technology, USA), mouse antibodies against glial fibrillary acidic protein (GFAP; astrocytic marker, 1:500; Cell Signaling Technology, USA), rabbit monoclonal antibodies against neuron-specific nuclear protein (NeuN; neuronal marker, 1:300; Abcam, England), rabbit anti-Iba1 (microglia marker, 1:200; Affinity Biosciences, USA), mouse anti-calcitonin gene-related peptide (CGRP; 1:200; Abcam, England), FIT4-conjugated isolectin B4 (IB4; 1:100; Sigma, L2895, USA), mouse anti-neurofilament-200 (NF200; 1:200; Sigma, USA), and mouse anti-Gelsolin (GS; 1:100; Millipore, USA). The specificities of antibodies were checked by omitting the primary antibody during immunostaining as well as during western blotting.

2.9 | Statistical analyses

All of the data are presented as the mean \pm SD. Data were analyzed using GraphPad Prism 5.0 (GraphPad Software Inc., La Jolla, CA). The data from behavioral tests were statistically analyzed by two-way analyses of variance (ANOVAs). Comparisons of more than two

groups were made using one-way ANOVAs with Tukey post hoc tests for pairwise comparisons. A $p < 0.05$ was considered statistically significant.

3 | RESULTS

3.1 | SMIR induces mechanical allodynia in rats

We chose the SMIR rat model for investigating CPSP. Consistent with previous reports, SMIR surgery-induced prolonged mechanical allodynia in the ipsilateral hind paw of each rat compared with that in the sham group (Figure 1a). At baseline, the PWT to mechanical stimulation of the ipsilateral hind paw was approximately 15 g, while the post-SMIR PWT gradually decreased to a minimum of 5.67 ± 0.72 g at 10 d after SMIR ($p < 0.001$), after which it gradually recovered toward normal levels. As shown in Figure 1a, the PWT reached 16.39 ± 0.67 g at 20 d after SMIR, which was significantly different compared with that of the sham group; in contrast, there was no significant difference in the PWT on the contralateral side between these two groups at this time (Figure 1a). However, SMIR had no effect on thermal hyperalgesia (Figure 1b). These behavioral results are consistent with previous reports (Flatters, 2008), verifying the successful establishment of the SMIR rat model in our present study.

3.2 | SMIR induces upregulation of TLR4 and CD11b in the spinal dorsal horn

In the central nervous system, TLR4 is expressed in microglia and is involved in microglial activation. To evaluate the effect of TLR4 on microglia in the spinal dorsal horn of SMIR rats, TLR4 and CD11b, a marker for microglial activation, were measured by qRT-PCR and western blotting. The results showed that both mRNA and protein expression levels of TLR4 were significantly increased in the spinal cord dorsal horn beginning at day 5, reached a peak at day 10, and lasted until day 15 after SMIR surgery (Figure 1c,e). SMIR surgery also led to enhanced expression of CD11b in the dorsal horn (Figure 1d,f). Similar to those of TLR4, both mRNA and protein expression levels of CD11b were increased at 5-d post-surgery and reached a peak at 10 d after SMIR surgery. However, both mRNA and protein expression levels of CD11b returned to normal at 15 d after SMIR surgery, as they were not significantly different compared with those of the sham group. These results suggest that microglia play a role in the early stage but not the late stage of CPSP induced by SMIR.

3.3 | TLR4 is widely expressed in microglia and neurons within the spinal cord

We used double immunofluorescent staining to determine the distribution of TLR4 in the spinal cords of naïve rats. The results

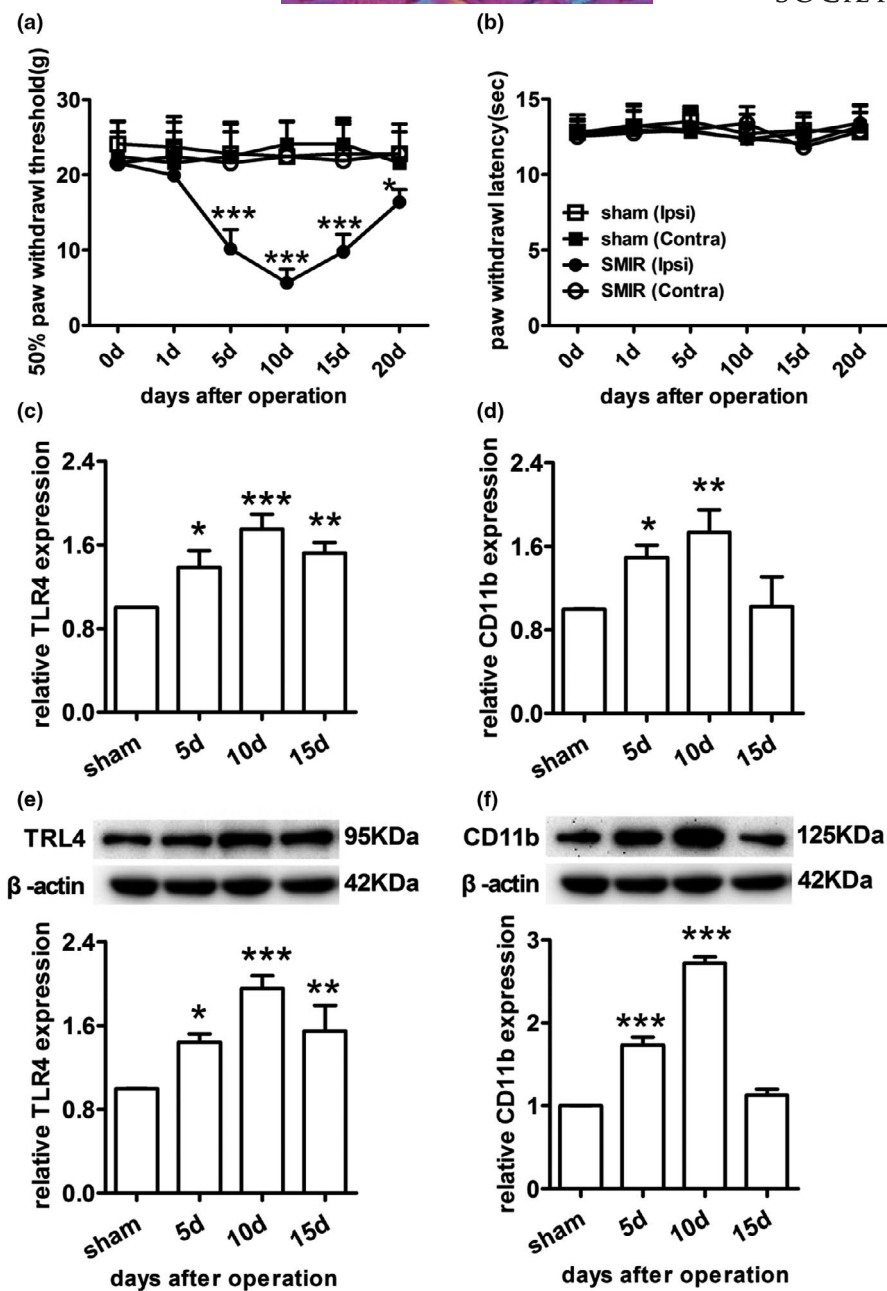


FIGURE 1 Effects of SMIR surgery on the expression of TLR4 and CD11b in the ipsilateral spinal dorsal horn. (a) The PWTs of the ipsilateral but not contralateral hind paws of SMIR rats were significantly reduced. (b) SMIR surgery did not induce any change in thermal hyperalgesia in either hind paw. (c) Expression of TLR4 mRNA was increased in the ipsilateral spinal dorsal horn of SMIR rats. (d) Expression of CD11b mRNA was increased in the ipsilateral spinal dorsal horn of SMIR rats. (e) Representative western blotting and corresponding graph showing that TLR4 protein expression was increased in the ipsilateral spinal dorsal horn of SMIR rats; β -actin served as a loading control. (f) Representative western blotting and corresponding graph showing that CD11b protein expression was increased in the ipsilateral spinal dorsal horn of SMIR rats; β -actin served as a loading control. Data were presented as means \pm SD. Sham, rats underwent only skin incisions 15 days prior to tissue collection. SMIR, rats underwent skin incisions and muscle retraction. 5d, rats underwent SMIR surgery 5 days prior to tissue collection. 10d, rats underwent SMIR surgery 10 days prior to tissue collection. 15d, rats underwent SMIR surgery 15 days prior to tissue collection. Ipsi, ipsilateral. Contra, contralateral. The data from behavioral tests were statistically analyzed by two-way ANOVAs. $n = 6$ rats per group. $***p < 0.001$ versus sham. Statistical differences for western blotting data were determined by one-way ANOVAs with Tukey post hoc tests. $n = 3$ rats per group. $*p < 0.05$, $**p < 0.01$, $***p < 0.001$ versus sham

showed that TLR4 was co-localized with NeuN, a specific marker for neurons, (Figure 2a-c), and Iba1, a specific marker of microglia, (Figure 2d-f), but not with GFAP, a specific marker of astrocytes,

(Figure 2g-i), in the dorsal horn. These data suggest that TLR4 is widely expressed in a variety of cells within the spinal cord of naïve rats except astrocytes.

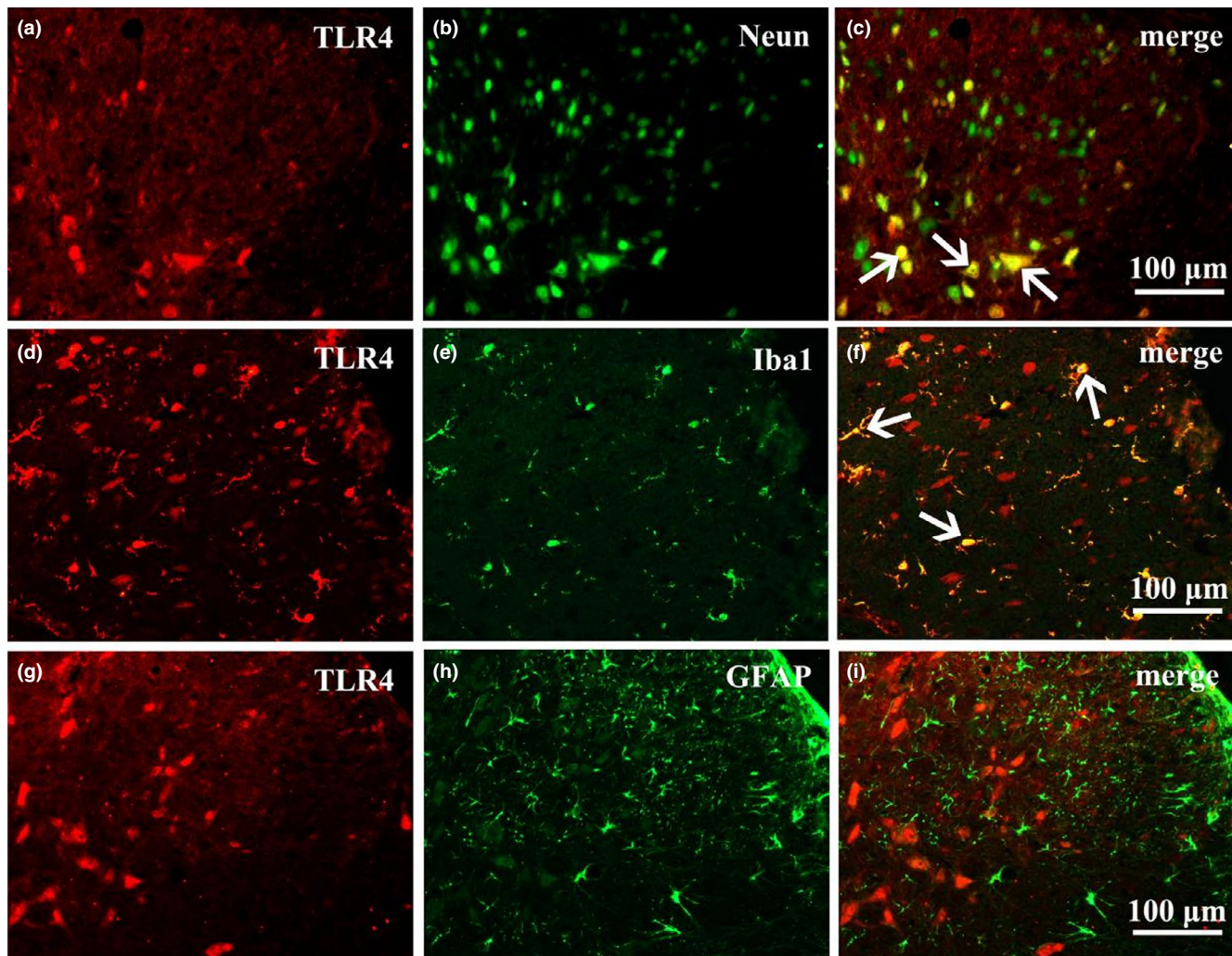


FIGURE 2 The distribution of TLR4 in the spinal dorsal horn of naïve rats. Representative pictures showing that TLR4 is co-localized with NeuN, a specific marker for neurons (a–c) and Iba1, a specific marker of microglia (d–f) (arrows), but not with GFAP, a specific marker of astrocytes (g–i). $n = 3$ rats. Scale bars: 100 μm

3.4 | TLR4 regulates SMIR-induced activation of spinal microglia by NF- κB

To determine the effect of TLR4 on SMIR-induced persistent pain in the central nervous system, we examined the activation of spinal microglia following intrathecal injection of LPS-RS, a TLR4 antagonist, in SMIR rats. The results showed that the 50% PWT of SMIR rats after LPS-RS administration was significantly increased compared with that of SMIR rats injected with saline, which effectively alleviated SMIR-induced mechanical hyperalgesia (Figure 3a). In the spinal cord, the injection of LPS-RS resulted in a significant decrease in the downstream molecule of TLR4, NF- κB , indicating that LPS-RS effectively inhibited the function of TLR4 (Figure 3b). In addition, CD11b, a marker of microglial activation, was also significantly reduced following LPS-RS injection as compared with that in SMIR rats injected with saline, indicating that inhibition of TLR4 in the spinal cord inhibited the microglial activation in SMIR rats (Figure 3c).

To further investigate the activation of microglia by TLR through NF- κB in SMIR-induced CPSP, we intrathecally administered the NF- κB inhibitor, PDTC, to SMIR rats. Compared with the results in SMIR rats injected with saline, PDTC injections effectively inhibited NF- κB expression (Figure 3e), alleviated SMIR-induced mechanical hyperalgesia (Figure 3d), and reduced the expression of CD11b in the spinal cord (Figure 3f). These results suggest that the TLR4/NF- κB signaling pathway activates microglia to participate in SMIR-induced CPSP.

3.5 | TLR4 is widely expressed in neurons but not satellite glial cells in DRGs

It has been reported that TLR4 is expressed not only in the central nervous system, but also in the peripheral nervous system (Bai et al., 2014; Bruno et al., 2018). Indeed, we found that TLR4 expression was also detected in normal rat DRGs, as indicated by double immunofluorescent staining. As shown in Figure 5, TLR4 was co-localized

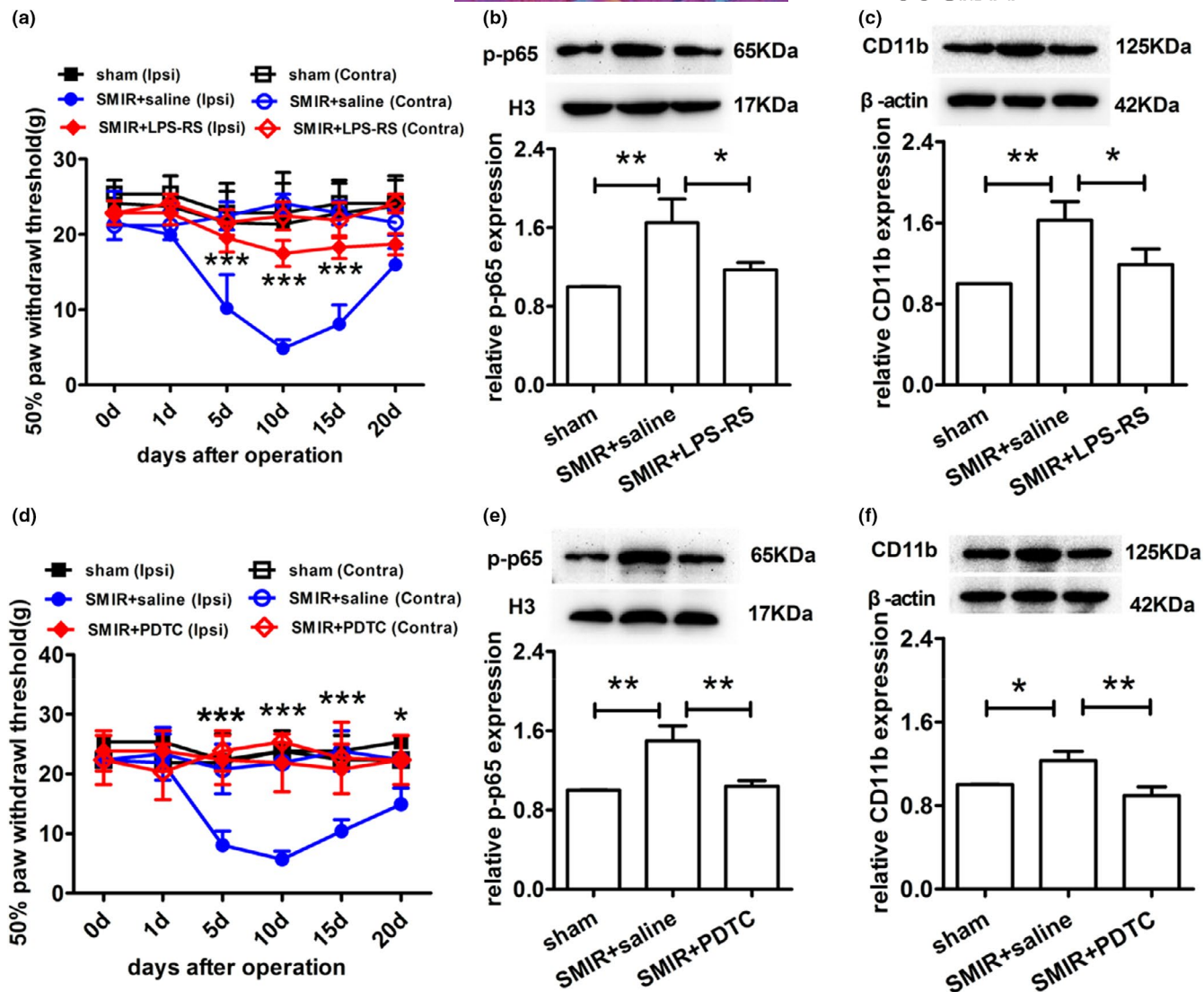


FIGURE 3 Effects of the TLR4/NF- κ B signaling pathway on microglia in SMIR rats. (a) Intrathecal injection of LPS-RS alleviated mechanical hyperalgesia in SMIR rats. (b) Representative western blotting and corresponding graph showing that NF- κ B protein expression was decreased in the ipsilateral spinal dorsal horn of SMIR rats on day 10 after surgery following intrathecal injection of LPS-RS; H3 served as a loading control. (c) Representative western blotting and corresponding graph showing that CD11b was reduced in the ipsilateral spinal dorsal horn of SMIR rats on day 10 after surgery following intrathecal injection of LPS-RS; β -actin served as a loading control. (d) Intrathecal injection of PDTC alleviated mechanical hyperalgesia in SMIR rats. (e) Representative western blotting and corresponding graph showing that NF- κ B protein expression was decreased in the ipsilateral spinal dorsal horn of SMIR rats on day 10 after surgery following intrathecal injection of PDTC; H3 served as a loading control. (f) Representative western blotting and corresponding graph showing that CD11b was reduced in the ipsilateral spinal dorsal horn of SMIR rats on day 10 after surgery following intrathecal injection of PDTC; β -actin served as a loading control. Data were presented as means \pm SD. Sham, rats underwent only skin incisions without muscle retraction. SMIR+saline, rats undergoing SMIR surgery were injected with saline. SMIR+LPS-RS, rats undergoing SMIR surgery were injected with LPS-RS. SMIR+PDTC, rats undergoing SMIR surgery were injected with PDTC. Ipsi, ipsilateral. Contra, contralateral. The data from behavioral tests were statistically analyzed by two-way ANOVAs. $n = 5-6$ rats per group. * $p < 0.05$, ** $p < 0.01$, *** $p < 0.001$ versus SMIR+saline. The data from western blotting were statistically analyzed by one-way ANOVAs with Tukey post hoc tests. $n = 3$ rats per group. * $p < 0.05$, ** $p < 0.01$, *** $p < 0.001$ versus SMIR+saline

with either CGRP, a marker of peptidergic neurons (Figure 4a-c), IB4, a marker of a fraction of small, nonmyelinated nociceptive neurons (Figure 4d-f), or NF200, a marker of large, myelinated non-nociceptive neurons (Figure 4g-i). However, TLR4 was not co-localized with GS, a marker of satellite glial cells (Figure 4j-l). These data suggest that TLR4 is widely expressed in all sizes of neurons in DRGs, but not in satellite glial cells.

3.6 | SMIR induces upregulation of TLR4 and Nav1.7 in DRGs

In the present study, we found that TLR4 was involved in SMIR-induced nociception in the spinal cord by activating microglia. However, TLR4 was not expressed in satellite glial cells within DRGs. Therefore, we hypothesized that the mechanism of peripheral involvement of TLR4

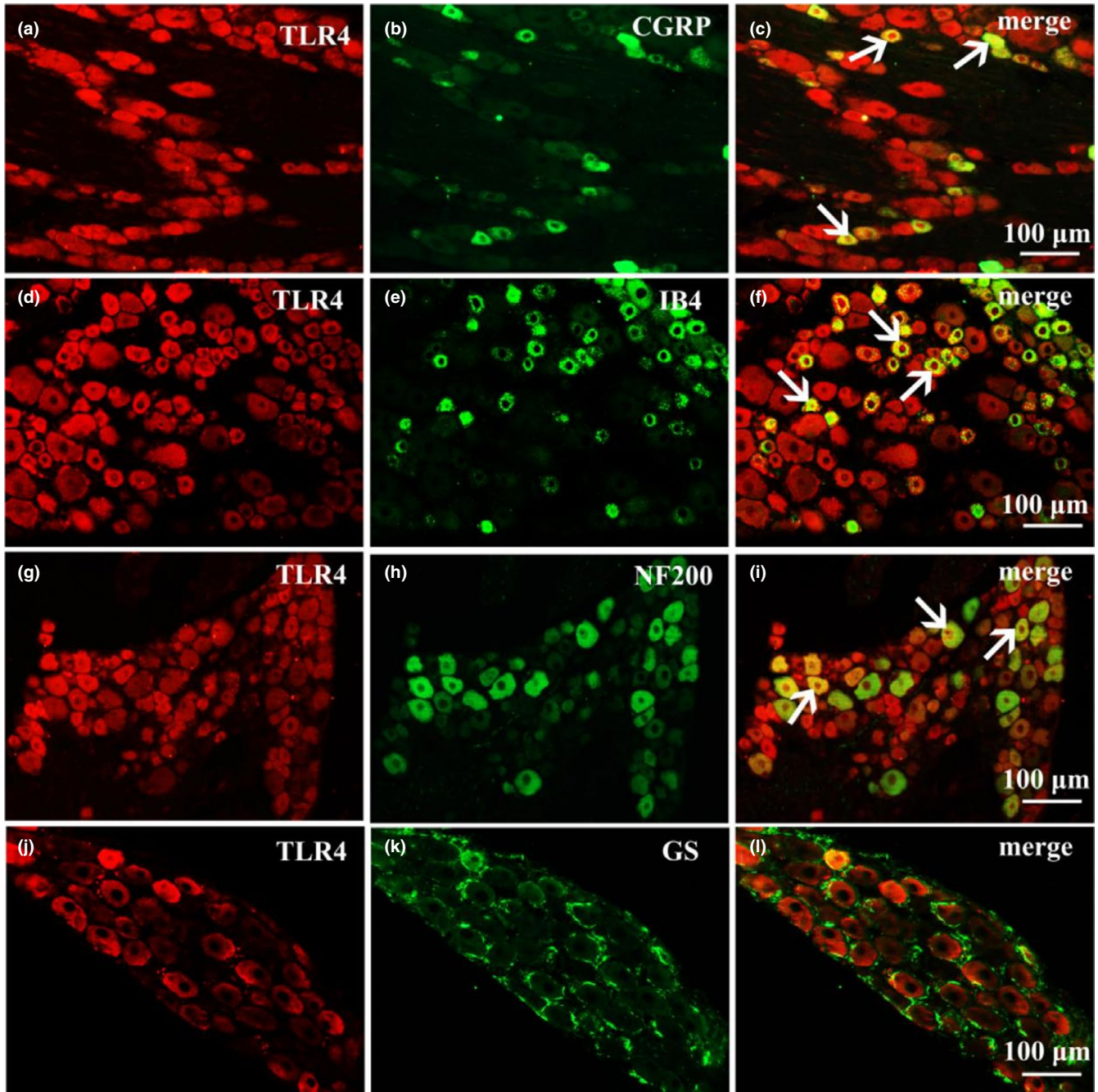


FIGURE 4 The distribution of TLR4 in DRGs of naïve rats. Representative pictures showing that TLR4 was co-localized with CGRP, a marker of peptidergic neurons (a–c), IB4, a marker of a fraction of small, nonmyelinated nociceptive neurons (d–f) and NF200, a marker of large, myelinated non-nociceptive neurons (g–i) (arrows), but not with GS, a marker of satellite glial cells (j–l). $n = 3$ rats per group. Scale bars: 100 μm

in SMIR-induced CPSP is distinct from that in the central nervous system. To determine whether SMIR surgery-induced changes in TLR4 within DRGs, we measured mRNA and protein levels of TLR4 in DRGs in SMIR rats. Because the NF- κB signaling pathway may regulate the expression of Nav1.7 in DRG neurons (Huang et al., 2014; Xie et al., 2019), we simultaneously measured the expression of Nav1.7 within DRGs of SMIR rats. As shown in Figure 6, compared with those in the sham group, both mRNA and protein levels of TLR4 (Figure 5a,c) and Nav1.7 (Figure 5b,d) were significantly increased in the DRGs of SMIR rats starting at 5 d after surgery, peaked at 10 d, and continued

until 15 d after surgery. In addition, we found that TLR4 and Nav1.7 were co-localized in naïve rat DRG neurons (Figure 5e–g), thus, indicating their possible interaction.

3.7 | TLR4 regulates Nav1.7 expression through NF- κB in DRGs to participate in SMIR-induced CPSP

To investigate the regulation of TLR4 on Nav1.7 within DRGs of SMIR rats, we suppressed the function of TLR4 by intrathecal injection of

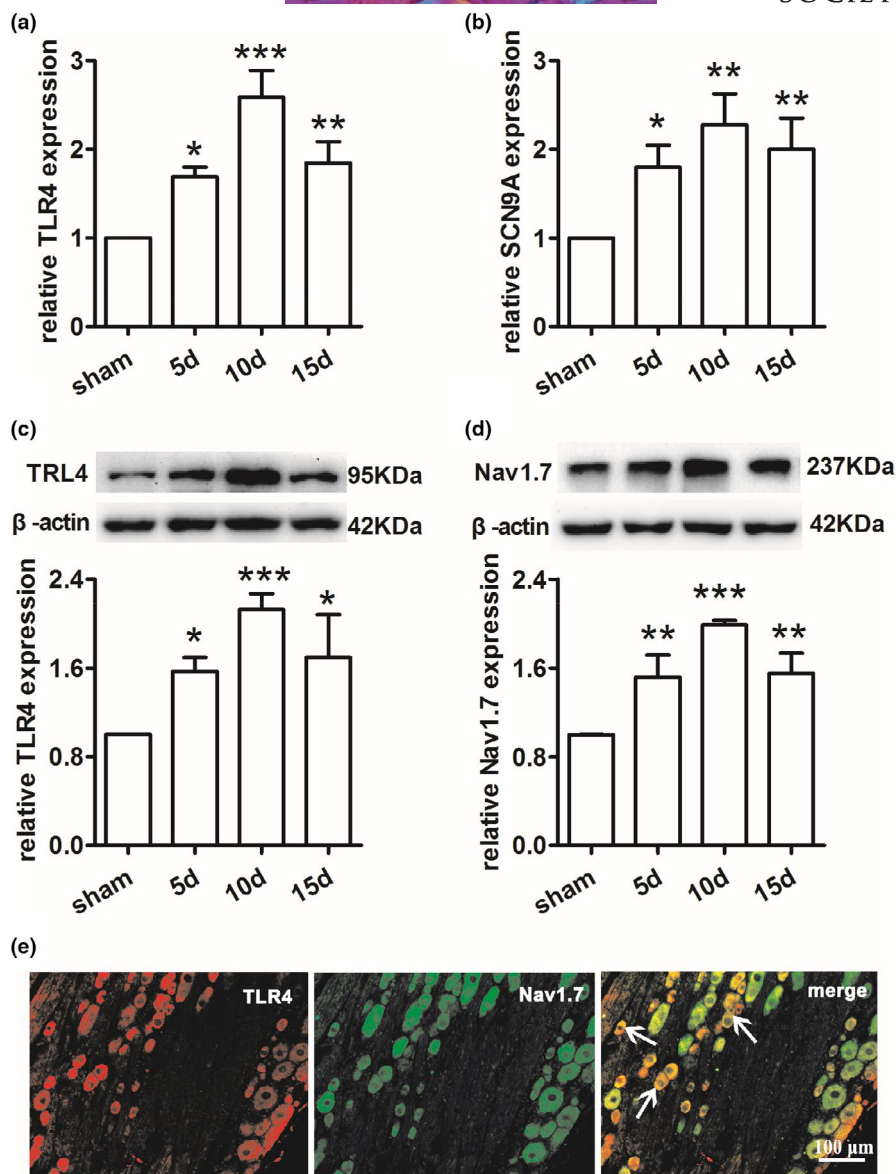


FIGURE 5 Effects of SMIR surgery on TLR4 and Nav1.7 in ipsilateral DRGs. (a) Expression of TLR4 mRNA was increased in the ipsilateral DRGs of SMIR rats. (b) Expression of Nav1.7 mRNA was increased in the ipsilateral DRGs of SMIR rats. (c) Representative western blotting and corresponding graph showing that TLR4 protein expression was increased in the ipsilateral DRGs of SMIR rats; β -actin served as a loading control. (d) Representative western blotting and corresponding graph showing that Nav1.7 protein expression was increased in the ipsilateral DRGs of SMIR rats; β -actin served as a loading control. (e–g) The immunofluorescence staining pictures showing that TLR4 was co-localized with Nav1.7 in DRGs of naïve rats. (arrows). Scale bars: 100 μ m. Data were presented as means \pm SD. Sham, rats underwent only skin incisions without muscle retraction. 5d, rats underwent SMIR surgery 5 days prior to tissue collection. 10d, rats underwent SMIR surgery 10 days prior to tissue collection. 15d, rats underwent SMIR surgery 15 days prior to tissue collection. $n = 3$ rats per group. Statistical differences were determined by one-way ANOVAs with Tukey post hoc tests. * $p < 0.05$, ** $p < 0.01$, *** $p < 0.001$ versus sham

LPS-RS. We found that inhibition of TLR4 not only inhibited NF- κ B expression in DRGs (Figure 6a), but also led to a decrease in Nav1.7 expression (Figure 6b). Similarly, Nav1.7 was also significantly reduced after intrathecal injection of PDTC, a NF- κ B inhibitor, compared with that in SMIR rats injected with saline (Figure 6c,d). These data suggest that the TLR4/NF- κ B signaling pathway regulates the expression of Nav1.7 in DRGs of SMIR rats, possibly to trigger peripheral hyperalgesia.

3.8 | Intrathecal injection of LPS-RS and PDTC had no effect upon naïve rats

To definitely show the effect of LPS-RS and PDTC is attenuating allodynia not just increasing sensory thresholds in general, but also we detected the effect of the drugs upon naïve rats. The results showed that LPS-RS and PDTC had no effect on mechanical sensitivity of naïve rats (Figure 7a,f), nor did they cause changes of related

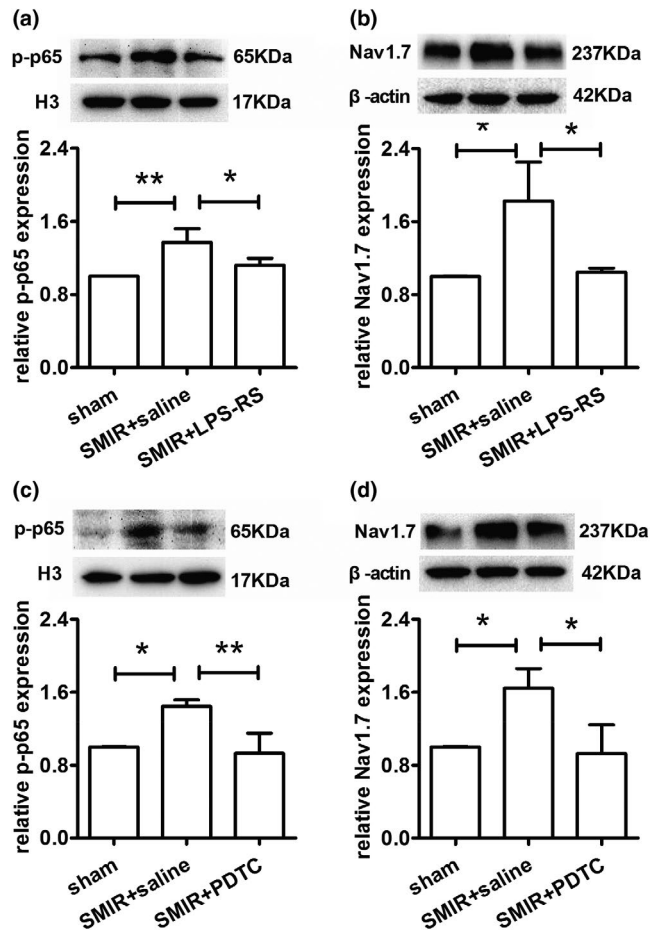


FIGURE 6 The TLR4/NF- κ B signaling pathway regulates the expression of Nav1.7 in DRGs of SMIR rats. (a) Representative western blotting and corresponding graph showing that NF- κ B protein expression was decreased in DRGs of SMIR rats with intrathecal injection of LPS-RS ($n = 3$; $*p < 0.05$, $**p < 0.01$) compared with that in SMIR rats injected with saline; H3 served as a loading control. (b) Representative western blotting and corresponding graph showing that Nav1.7 expression was reduced in DRGs of SMIR rats with intrathecal injection of LPS-RS ($n = 3$; $*p < 0.05$) compared with that in SMIR rats injected with saline; β -actin served as a loading control. (c) Representative western blotting and corresponding graph showing that NF- κ B protein expression was decreased in DRGs of SMIR rats with intrathecal injection of PDTC ($n = 3$; $*p < 0.05$, $**p < 0.01$) compared with that in SMIR rats injected with saline; H3 served as a loading control. (d) Representative western blotting and corresponding graph showing that Nav1.7 expression was decreased in DRGs of SMIR rats with intrathecal injection of PDTC ($n = 3$; $*p < 0.05$) compared with that in SMIR rats injected with saline; β -actin served as a loading control. Data were presented as means \pm SD. Sham, rats underwent only skin incisions without muscle retraction. SMIR+saline, rats undergoing SMIR surgery were injected with saline. SMIR+LPS-RS, rats undergoing SMIR surgery were injected with LPS-RS. SMIR+PDTC, rats undergoing SMIR surgery were injected with PDTC. $n = 3$ rats per group. Statistical differences were determined by one-way ANOVAs with Tukey post hoc tests. $*p < 0.05$, $**p < 0.01$, $***p < 0.001$ versus SMIR+saline

proteins, which include p-p65 (Figure 7b,g) and CD11b (Figure 7c,h) in the spinal cord, and p-p65 (Figure 7d,i) and Nav1.7 (Figure 7e,j) in DRG.

3.9 | Activation of TLR4 in naïve rats results in activation of spinal microglia and upregulation of Nav1.7 in DRGs

Naïve rats were intrathecally injected with different doses of LPS to activate TLR4. The results showed that 0.5 μ g/ μ l of LPS did not induce mechanical hyperalgesia and did not activate NF- κ B (Figure 7a). In contrast, injection of 1.0 or 2.0 μ g/ μ l of LPS not only induced mechanical hyperalgesia (Figure 8a), but also significantly increased NF- κ B expression in both the spinal cord (Figure 8b) and within DRGs (Figure 8d) as well as increased CD11b expression in the spinal cord (Figure 8c) and Nav1.7 expression within DRGs (Figure 8e). These results suggest that activation of TLR4 may induce mechanical hyperalgesia, activate central microglia, and promote the expression of Nav1.7 in DRGs.

4 | DISCUSSION

CPSP represents a widespread clinical problem to both patients and doctors. To elucidate the mechanisms of CPSP, we used an SMIR rat model and explored the central and peripheral mechanisms of TLR4/NF- κ B signaling pathways in SMIR-induced CPSP.

CPSP can occur following various types of surgery. In addition to skin incisions, muscle damage, and inflammatory responses in surgical regional tissues, there is also a common feature during surgery consisting of a long period of tissue retraction. Therefore, we used an SMIR rat model to simulate surgical procedures that typically induce CPSP. Consistent with a previous report by Flatters et al. (Flatters, 2008), we found that SMIR surgery produced mechanical hyperalgesia but not thermal hyperalgesia.

Neuroinflammation plays an important role in the occurrence and maintenance of pain. The TLR4/NF- κ B signaling pathway is a classic and critical pathway involved in inflammatory responses and plays a role in many types of pain (Liu et al., 2012; Piao et al., 2018; Sun et al., 2018). Elisei et al. have reported that TLR4 is involved in SMIR-induced CPSP in the spinal cord, and inhibition of TLR4 can alleviate mechanical hypersensitivity caused by SMIR. However, they did not report the molecular mechanism by which spinal TLR4 is involved in SMIR-induced CPSP (Elisei et al., 2020). In the present study, we detected a significant increase in TLR4 expression in both the spinal cord and within DRGs of SMIR rats. Double immunofluorescent staining showed that TLR4 was expressed in microglia, and neurons within the spinal cord, which is consistent with previous reports (Tang et al., 2007). However, TLR4 was expressed in all sizes of neurons but not in satellite glial cells within DRGs, which is consistent with a previous report (Sun et al., 2019). Therefore, we hypothesize that the mechanism of TLR4 in SMIR-induced CPSP is likely different between the central and peripheral nervous systems.

Previous studies have reported that the TLR4 signaling pathway regulates the activation of microglia (Qin et al., 2005; Yang et al., 2018). Microglial activation is a key factor in central nervous

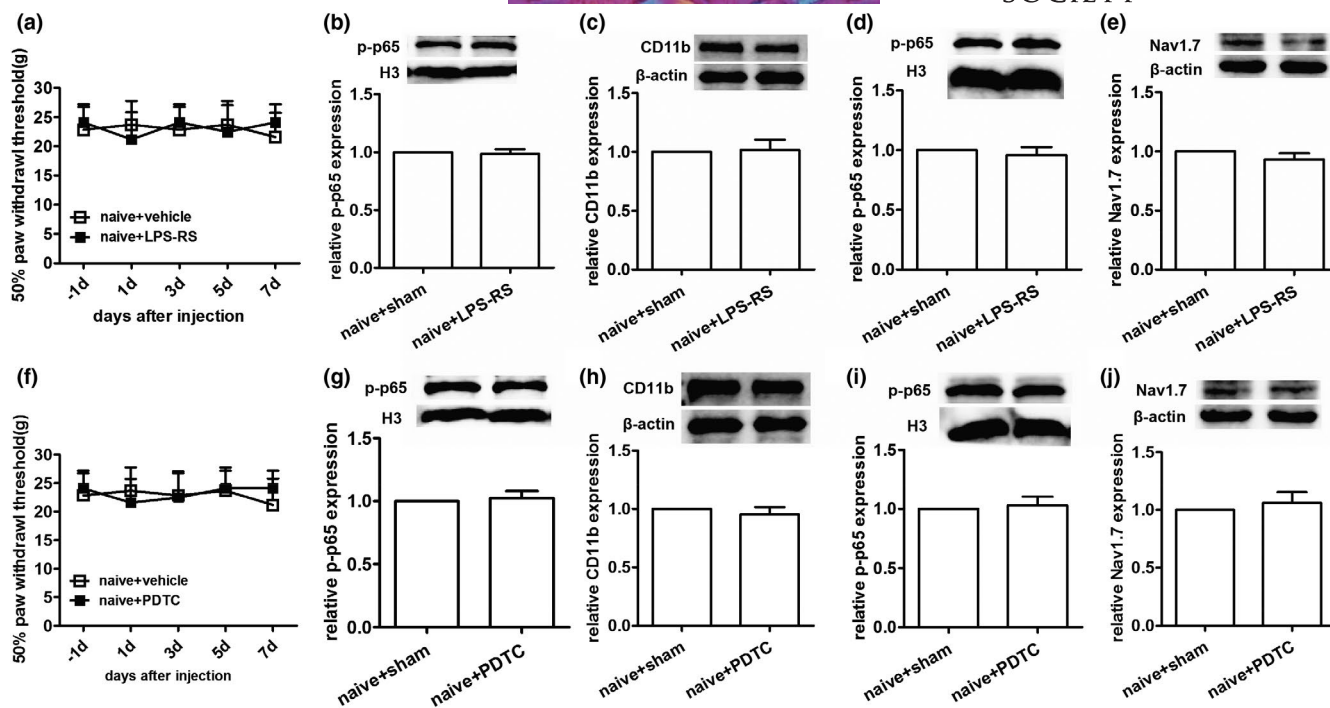


FIGURE 7 Intrathecal injection of LPS-RS and PDTC had no effect on mechanical sensitivity in naïve rats. (a) Mechanical sensitivity of rats injected with LPS-RS intrathecally. $n = 6$. (b–e) Representative western blotting bands and corresponding graph of p-p65 (spinal cord), CD11b (spinal cord), p-p65 (DRG), Nav1.7 (DRG) in rats injected with LPS-RS intrathecally. $n = 3$. (f) Mechanical sensitivity of rats injected with PDTC intrathecally. $n = 6$. (g–j) Representative western blotting bands and corresponding graph of p-p65 (spinal cord), CD11b (spinal cord), p-p65 (DRG), Nav1.7 (DRG) in rats injected with PDTC intrathecally. Tissue materials for western blotting were obtained on the 7th day after injection. $n = 3$

system during pain (Ji et al., 2013; Old et al., 2015; Zhang et al., 2005). Therefore, we first examined the effect of TLR4 on microglia in the spinal cords of SMIR rats. We found that SMIR surgery led to a significant increase in the expression levels of TLR4 and CD11b, a marker of microglial activation, indicating increased microglial activation. Interestingly, CD11b was most highly expressed at 10 d after SMIR and returned to normal levels at 15 d after SMIR, suggesting that activated microglia were only involved in the early stage of SMIR-induced CPSP and were not associated with the maintenance of later stages. This finding is consistent with previous reports demonstrating that microglia are involved in early neuropathic pain induced by nerve injury (Naseri et al., 2013). In the present study, administration of a TLR4 antagonist (LPS-RS) significantly decreased the expression levels of NF- κ B (a downstream molecule of TLR4) and CD11b in the spinal cords of SMIR rats; furthermore, this manipulation of administration of a TLR4 antagonist ameliorated SMIR-induced CPSP, which is consistent with a previous report by Christianson et al. (Christianson et al., 2011). These results suggest that the TLR/NF- κ B signaling pathway in the spinal cord is involved in SMIR-induced CPSP and likely induces hyperalgesia by activating microglia. To further test our hypothesis, we inhibited NF- κ B in SMIR rats, and the results showed that the expression of CD11b was significantly decreased while pain was relieved, indicating that NF- κ B regulates the activation of microglia in SMIR-induced CPSP. In contrast, spinal application of a TLR4 agonist (LPS) resulted in an increase in CD11b expression and in

microglial activation in naïve rats. We also found that LPS was sufficient to induce pain behaviors in naïve rats, which is consistent with a previous report (Loram et al., 2011). Therefore, our findings demonstrate that SMIR surgery leads to activation of the TLR/NF- κ B signaling pathway, which further promotes the activation of microglia to exacerbate hypersensitivity of pain.

However, as can be seen from Figure 2, activated microglia were significantly reduced at 15 d after SMIR surgery, whereas mechanical hyperalgesia was still persistent, and the expression of TLR4 was still significantly upregulated in the spinal cord. This discrepancy may be explained by the following. In the present study, TLR4 was expressed not only in microglia, but also in neurons within the spinal cord. Hence, we speculate that TLR4 may be involved in pain maintenance by acting on neurons in the later stage of SMIR-induced CPSP, which we plan to investigate in our future experiments.

TLR4 is expressed not only in the central nervous system, but also in the peripheral nervous system (Bruno et al., 2018; Xu et al., 2018). TLR4/NF- κ B signaling pathway in the peripheral nervous system has been reported to play an important role in postoperative pain. Erika Ivanna Araya et al. found that activation of TLR4/NF- κ B signaling pathway in the trigeminal ganglion contributes to the development of facial heat and mechanical hyperalgesia (Araya et al., 2020). TLR4/NF- κ B signaling activation in local injured tissue and DRG contribute to the development of postoperative pain induced by plantar incision in rat hind paw via regulating

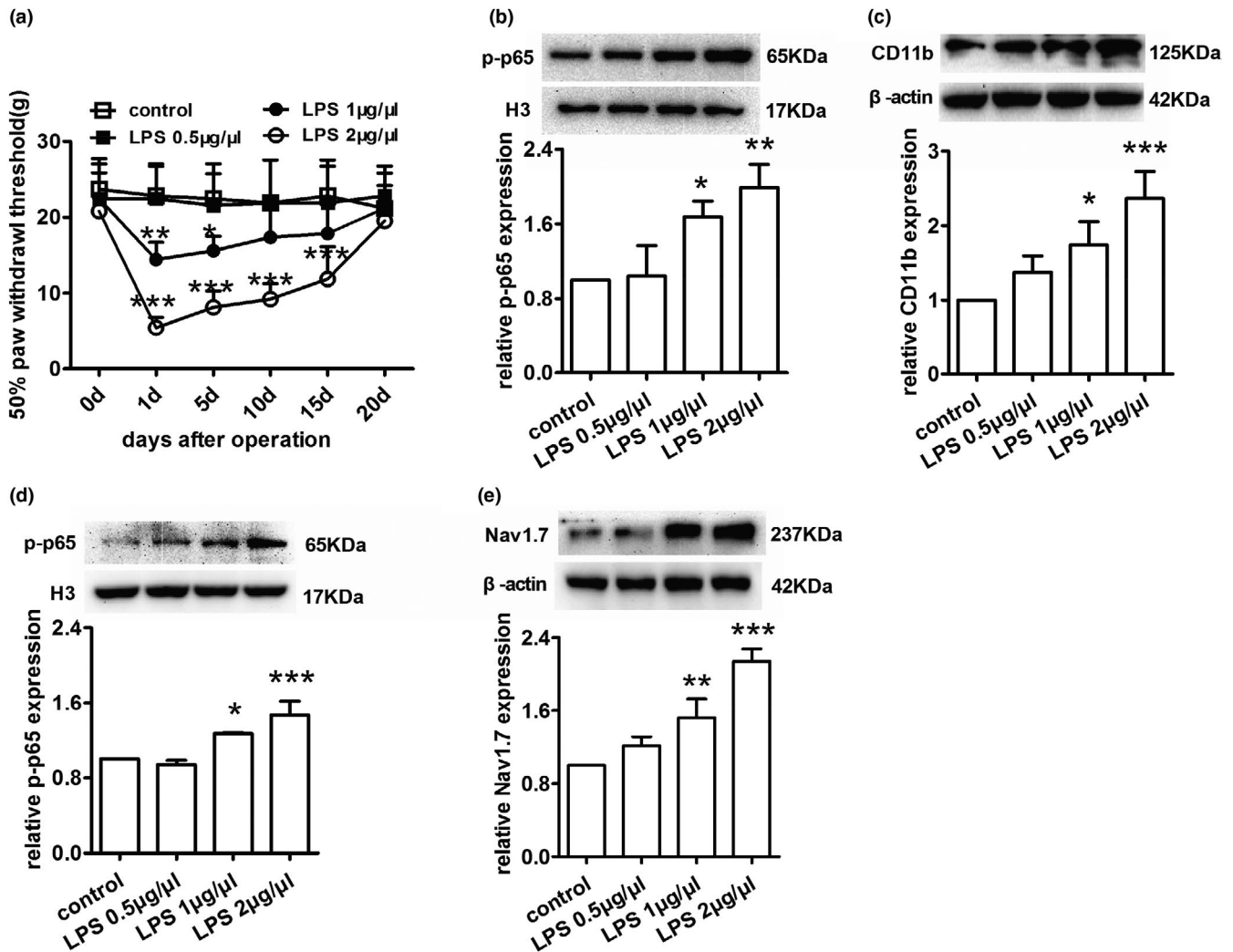


FIGURE 8 Intrathecal injection of LPS results in activation of spinal microglia and upregulation of Nav1.7 in DRGs of naïve rats. (a) Intrathecal injection of LPS-induced mechanical hyperalgesia in naïve rats. (b, d) Representative western blotting and corresponding graph showing that NF- κ B protein expression was increased in the spinal dorsal horn (b) and within DRGs (d) of naïve rats with intrathecal injection of LPS; H3 served as a loading control. (c) Representative western blotting and corresponding graph showing that CD11b expression was increased in the spinal dorsal horn of naïve rats with intrathecal injection of LPS; β -actin served as a loading control. (e) Representative western blotting and corresponding graph showing that Nav1.7 expression was increased in DRGs of naïve rats with intrathecal injection of LPS; β -actin served as a loading control. Data were presented as means \pm SD. Control, rats were injected with saline. LPS 0.5 μ g/ μ l, rats were injected with LPS (0.5 μ g/ μ l, 10 μ l). LPS 1 μ g/ μ l, rats were injected with LPS (1 μ g/ μ l, 10 μ l). LPS 2 μ g/ μ l, rats were injected with LPS (2 μ g/ μ l, 10 μ l). The data from behavioral tests were statistically analyzed by two-way ANOVAs. $n = 6$ rats per group. * $p < 0.05$, ** $p < 0.01$, *** $p < 0.001$ versus control. The data from western blotting were statistically analyzed by one-way ANOVAs with Tukey post hoc tests. $n = 3$ rats per group. * $p < 0.05$, ** $p < 0.01$, *** $p < 0.001$ versus control

pro-inflammatory cytokines release (Xing et al., 2018). However, the molecular mechanism of peripheral TLR4/NF- κ B signaling pathway in SMIR-induced CPSP remains unclear. Since TLR4 activates microglia in the central nervous system, we speculate that it is possible that TLR4 also participates in SMIR-induced CPSP in the peripheral nervous system by regulating glial activation. However, as previously mentioned, we found that TLR4 was expressed in all sizes of neurons, but not in satellite glial cells within DRGs. Therefore, TLR4 is unlikely to participate in SMIR-induced CPSP in the peripheral nervous system by regulating activation of satellite glial cells.

According to previous studies, NF- κ B increases neuronal excitability by regulating the expression of Nav1.7 in DRG neurons (Huang et al., 2014; Xie et al., 2019). In the present study, we found that Nav1.7 expression was upregulated in DRGs of SMIR rats. Moreover, Nav1.7 and TLR4 were co-expressed in DRG neurons. It is possible that this phenomenon is related to TLR4 activation. Furthermore, when the function of TLR4 was inhibited, the expression levels of NF- κ B and Nav1.7 were both reduced. Similarly, when PDTC was applied to inhibit NF- κ B, Nav1.7 expression was also reduced. We also found that LPS-activated TLR4, leading to the upregulation of Nav1.7 in DRGs, which also confirmed our hypothesis.

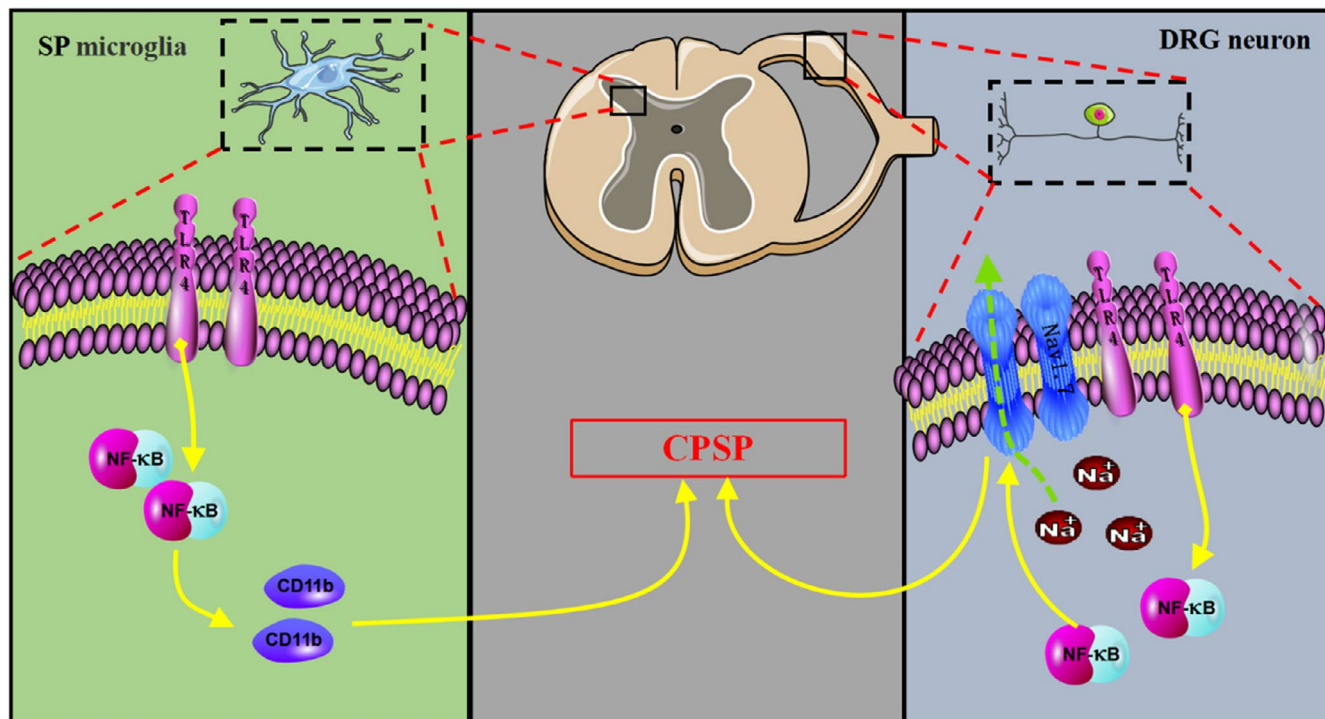


FIGURE 9 Schematic diagram of TLR4 participating in SMIR-induced CPSP mechanism

However, since we used intrathecal injection, the independent role of TLR4 in DRG cannot be ruled out. TLR4 /NF- κ B signaling pathway in the DRG and Spinal Cord might be participating in CPSP pain processing independently. What was exciting, of course, was that the discovery of the peripheral mechanism of CPSP that TLR4 regulates Nav1.7 in DRGs may represent a significant finding. As key components of resting membrane potentials and action potentials, sodium channels are considered as potential therapeutic targets for pain medication (Bennett et al., 2019). Additionally, targeting ion-channel protein changes in primary neurons is an important strategy for interference and treatment of pain (Dib-Hajj & Waxman, 2019). Our present study provides experimental evidence for a mechanism of sodium channels involved in SMIR-induced CPSP. Although our present study did not clarify the specific mechanism of NF- κ B in regulating Nav1.7 expression, we will investigate this phenomenon in future studies. In addition, although TLR4 is not expressed in satellite glial cells, TLR4 is expressed in DRG macrophages (Yu et al., 2020). This study does not rule out the possibility that TLR4 in macrophages within DRG may be involved in CPSP. Could TLR4 in macrophages regulate Nav1.7 in neurons to affect CPSP? This will be another exploration.

In summary, our present study demonstrated that the central and peripheral TLR4/NF- κ B signaling pathway is involved in the hyperalgesia of SMIR-induced CPSP through distinct mechanisms (Figure 9). In the peripheral nervous system, TLR4 upregulated expression of Nav1.7 in peripheral DRGs through downstream NF- κ B in SMIR-induced CPSP. In contrast, the TLR/NF- κ B signaling pathway in the spinal cord-activated microglia in SMIR-induced CPSP. Ultimately, our findings

demonstrate that activation of the peripheral and central TLR4/NF- κ B signaling pathway involved in the development of SMIR-induced CPSP.

CONFLICT OF INTEREST

The authors declare no conflict of interest.

AUTHOR CONTRIBUTIONS

Participated in research design: Cao, Z. Li, Xu, Zhu. Conducted experiments: Han, Shao, Ren, Y. Li. Performed data analyses: Shao, Han, Yu, Lin, L. Li, Sun. Wrote or contributed to the writing of the manuscript: Shao, Han, Cao, Z. Li, Luo, Zhu.

ORCID

Jing Cao  <https://orcid.org/0000-0003-3124-4780>

REFERENCES

- Araya, E.I., Barroso, A.R., Turnes, J.M., Radulski, D.R., Jaganaught, J.-R., Zampronio, A.R. et al. (2020) Toll-like receptor 4 (TLR4) signaling in the trigeminal ganglion mediates facial mechanical and thermal hyperalgesia in rats. *Physiology & Behavior*, 226, 113127.
- Bai, L., Zhai, C., Han, K., Li, Z., Qian, J., Jing, Y. et al. (2014) Toll-like receptor 4-mediated nuclear factor- κ B activation in spinal cord contributes to chronic morphine-induced analgesic tolerance and hyperalgesia in rats. *Neurosci Bull*, 30, 936–948.
- Bennett, D.L., Clark, A.J., Huang, J., Waxman, S.G. & Dib-Hajj, S.D. (2019) The role of voltage-gated sodium channels in pain signaling. *Physiological Reviews*, 99, 1079–1151.
- Bruno, K., Woller, S.A., Miller, Y.I., Yaksh, T.L., Wallace, M., Beaton, G. et al. (2018) Targeting toll-like receptor-4 (TLR4)-an emerging therapeutic target for persistent pain states. *Pain*, 159, 1908–1915.

- Chaplan, S.R., Bach, F.W., Pogrel, J.W., Chung, J.M. & Yaksh, T.L. (1994) Quantitative assessment of tactile allodynia in the rat paw. *Journal of Neuroscience Methods*, 53, 55–63.
- Christianson, C.A., Dumlaio, D.S., Stokes, J.A., Dennis, E.A., Svensson, C.I., Corr, M. et al. (2011) Spinal TLR4 mediates the transition to a persistent mechanical hypersensitivity after the resolution of inflammation in serum-transferred arthritis. *Pain*, 152, 2881–2891.
- Cox, J.J., Reimann, F., Nicholas, A.K., Thornton, G., Roberts, E., Springell, K. et al. (2006) An SCN9A channelopathy causes congenital inability to experience pain. *Nature*, 444, 894–898.
- Dib-Hajj, S.D. & Waxman, S.G. (2019) Sodium Channels in Human Pain Disorders: Genetics and Pharmacogenomics. *Annual Review of Neuroscience*, 42, 87–106.
- Dib-Hajj, S.D., Yang, Y. & Waxman, S.G. (2008) Genetics and molecular pathophysiology of Na(v)1.7-related pain syndromes. *Advances in Genetics*, 63, 85–110.
- Elisei, L.M.S., Moraes, T.R., Malta, I.H., Charlie-Silva, I., Sousa, I.M.O., Veras, F.P. et al. (2020) Antinociception induced by artemisinin nanocapsule in a model of postoperative pain via spinal TLR4 inhibition. *Inflammopharmacology*, 28, 1537–1551.
- Flatters, S.J. (2008) Characterization of a model of persistent postoperative pain evoked by skin/muscle incision and retraction (SMIR). *Pain*, 135, 119–130.
- Hargreaves, K., Dubner, R., Brown, F., Flores, C. & Joris, J. (1988) A new and sensitive method for measuring thermal nociception in cutaneous hyperalgesia. *Pain*, 32, 77–88.
- Huang, Y., Zang, Y., Zhou, L., Gui, W., Liu, X. & Zhong, Y. (2014) The role of TNF-alpha/NF-kappa B pathway on the up-regulation of voltage-gated sodium channel Nav1.7 in DRG neurons of rats with diabetic neuropathy. *Neurochemistry International*, 75, 112–119.
- Iwasaki, R., Matsuura, Y., Ohtori, S., Suzuki, T., Kuniyoshi, K. & Takahashi, K. (2013) Activation of astrocytes and microglia in the C3–T4 dorsal horn by lower trunk avulsion in a rat model of neuropathic pain. *Journal of Hand Surgery*, 38, 841–846.
- Ji, R.R., Berta, T. & Nedergaard, M. (2013) Glia and pain: is chronic pain a gliopathy? *Pain*, 154(Suppl 1), S10–28.
- Ji, R.R., Xu, Z.Z. & Gao, Y.J. (2014) Emerging targets in neuroinflammation-driven chronic pain. *Nature Reviews Drug Discovery*, 13, 533–548.
- Kehlet, H., Jensen, T.S. & Woolf, C.J. (2006) Persistent postsurgical pain: risk factors and prevention. *Lancet*, 367, 1618–1625.
- Li, L., Shao, J., Wang, J., Liu, Y., Zhang, Y., Zhang, M. et al. (2019) MiR-30b-5p attenuates oxaliplatin-induced peripheral neuropathic pain through the voltage-gated sodium channel Na(v)1.6 in rats. *Neuropharmacology*, 153, 111–120.
- Liu, T., Gao, Y.J. & Ji, R.R. (2012) Emerging role of Toll-like receptors in the control of pain and itch. *Neuroscience Bulletin*, 28, 131–144.
- Loram, L.C., Taylor, F.R., Strand, K.A., Frank, M.G., Sholar, P., Harrison, J.A. et al. (2011) Prior exposure to glucocorticoids potentiates lipopolysaccharide induced mechanical allodynia and spinal neuroinflammation. *Brain, Behavior, and Immunity*, 25, 1408–1415.
- Macrae, W.A. (2008) Chronic post-surgical pain: 10 years on. *British Journal of Anaesthesia*, 101, 77–86.
- Naseri, K., Saghaei, E., Abbaszadeh, F., Afhami, M., Haeri, A., Rahimi, F. et al. (2013) Role of microglia and astrocyte in central pain syndrome following electrolytic lesion at the spinothalamic tract in rats. *Journal of Molecular Neuroscience*, 49, 470–479.
- Old, E.A., Clark, A.K. & Malcangio, M. (2015) The role of glia in the spinal cord in neuropathic and inflammatory pain. *Handbook of Experimental Pharmacology*, 227, 145–170.
- Piao, Y., Gwon, D.H., Kang, D.-W., Hwang, T.W., Shin, N., Kwon, H.H. et al. (2018) TLR4-mediated autophagic impairment contributes to neuropathic pain in chronic constriction injury mice. *Molecular Brain*, 11, 11.
- Qin, L., Li, G., Qian, X., Liu, Y., Wu, X., Liu, B. et al. (2005) Interactive role of the toll-like receptor 4 and reactive oxygen species in LPS-induced microglia activation. *Glia*, 52, 78–84.
- Qu, R., Yao, F., Zhang, X., Gao, Y., Liu, T. & Hua, Y. (2019) SMN deficiency causes pain hypersensitivity in a mild SMA mouse model through enhancing excitability of nociceptive dorsal root ganglion neurons. *Scientific Reports*, 9, 6493.
- Raghavendra, V., Tanga, F. & DeLeo, J.A. (2003) Inhibition of microglial activation attenuates the development but not existing hypersensitivity in a rat model of neuropathy. *Journal of Pharmacology and Experimental Therapeutics*, 306, 624–630.
- Shao, J., Cao, J., Wang, J., Ren, X., Songxue, S.u., Li, M. et al. (2016) MicroRNA-30b regulates expression of the sodium channel Nav1.7 in nerve injury-induced neuropathic pain in the rat. *Molecular Pain*, 12.
- Størkson, R.V., Kjørsvik, A., Tjølsen, A. & Hole, K. (1996) Lumbar catheterization of the spinal subarachnoid space in the rat. *Journal of Neuroscience Methods*, 65, 167–172.
- Su, S., Shao, J., Zhao, Q., Ren, X., Cai, W., Li, L. et al. (2017) MiR-30b attenuates neuropathic pain by regulating voltage-gated sodium channel Nav1.3 in rats. *Frontiers in Molecular Neuroscience*, 10, 126.
- Sun, Q., Zhang, B.Y., Zhang, P.A., Hu, J., Zhang, H.H. & Xu, G.Y. (2019) Downregulation of glucose-6-phosphate dehydrogenase contributes to diabetic neuropathic pain through upregulation of toll-like receptor 4 in rats. *Molecular Pain*, 15, 1744806919838659.
- Sun, X., Zeng, H., Wang, Q., Yu, Q., Wu, J., Feng, Y. et al. (2018) Glycyrrhizin ameliorates inflammatory pain by inhibiting microglial activation-mediated inflammatory response via blockage of the HMGB1-TLR4-NF-kB pathway. *Experimental Cell Research*, 369, 112–119.
- Tang, S.-C., Arumugam, T.V., Xu, X., Cheng, A., Mughal, M.R., Jo, D.G. et al. (2007) Pivotal role for neuronal Toll-like receptors in ischemic brain injury and functional deficits. *Proceedings of the National Academy of Sciences of the United States of America*, 104, 13798–13803.
- Xie, M.-X., Zhang, X.-L., Xu, J., Zeng, W.-A., Li, D., Xu, T. et al. (2019) Nuclear Factor-kappaB Gates Na(v)1.7 Channels in DRG Neurons via Protein-Protein Interaction. *iScience*, 19, 623–633.
- Xing, F., Zhang, W., Wen, J., Bai, L., Gu, H., Li, Z. et al. (2018) TLR4/NF-kB signaling activation in plantar tissue and dorsal root ganglion involves in the development of postoperative pain. *Molecular Pain*, 14, 1744806918807050.
- Xu, J.T., Xin, W.J., Zang, Y., Wu, C.Y. & Liu, X.G. (2006) The role of tumor necrosis factor-alpha in the neuropathic pain induced by Lumbar 5 ventral root transection in rat. *Pain*, 123, 306–321.
- Xu, L., Liu, Y., Sun, Y., Li, H., Mi, W. & Jiang, Y. (2018) Analgesic effects of TLR4/NF-kB signaling pathway inhibition on chronic neuropathic pain in rats following chronic constriction injury of the sciatic nerve. *Biomedicine & Pharmacotherapy*, 107, 526–533.
- Yang, X., Zhang, J.D., Duan, L., Xiong, H.G., Jiang, Y.P. & Liang, H.C. (2018) Microglia activation mediated by toll-like receptor-4 impairs brain white matter tracts in rats. *Journal of Biomedical Research*, 32, 136–144.
- Yu, X., Liu, H., Hamel, K.A., Morvan, M.G., Yu, S., Leff, J. et al. (2020) Dorsal root ganglion macrophages contribute to both the initiation and persistence of neuropathic pain. *Nature Communications*, 11, 264.
- Zhang, R.-X., Liu, B., Wang, L., Ren, K.e., Qiao, J.-T., Berman, B.M. et al. (2005) Spinal glial activation in a new rat model of bone cancer pain produced by prostate cancer cell inoculation of the tibia. *Pain*, 118, 125–136.

How to cite this article: Han X, Shao J, Ren X, et al. The different mechanisms of peripheral and central TLR4 on chronic postsurgical pain in rats. *J Anat.* 2021;239:111–124. <https://doi.org/10.1111/joa.13406>